Available online at www.sciencedirect.com
SCIENCE DIRECT®
Cement & Concrete Composites 27 (2005) 131–140
Cement & Concrete Composites
www.elsevier.com/locate/cemconcomp

The fracture and fatigue performance in flexure of carbon fiber reinforced concrete

Zongcai Deng *

School of Civil and Architecture Engineering, Beijing University of Technology, Beijing 100022, PR China

Received 11 July 2003; accepted 9 March 2004

Abstract

The fracture parameters and fatigue performances of carbon fiber reinforced concrete is investigated by three point bending tests. In comparison with the results of quasi-static tests where no pre-cyclic loading is applied, the influence of pre-cyclic loading history on fracture parameters was researched by using compliance calibration. The test results show that the fracture parameters of carbon fiber reinforced concrete and plain concrete will be reduced if the pre-cyclic loading stress levels are higher than a certain threshold, and this threshold value for carbon fiber reinforced concrete is higher than that of plain concrete. The critical effective crack length for carbon fiber reinforced concrete is significantly larger than that of plain concrete and independent of the pre-cyclic loading history and fatigue life. Carbon fiber reinforced concrete has a considerable beneficial effect on the behaviour of concrete subjected to flexure fatigue loading.

Keywords: Concrete; Carbon fibers; Fracture parameters; Pre-cyclic loading history; Fatigue fracture life; Energy; Damage; Fracture; Composites

1. Introduction

In many civil engineering structures, concrete elements work with various types of cracks. The fracture energy of concrete depends on the loading history [1,2]. Consequently, it is necessary to predict the structure's life and fracture parameters for members which have had been suffered repeated loading in the past.

Concrete pavements for highways or bridge decks with cracks are subjected to a million cycles of repeated loading. Airport pavements are also subjected to many hundred thousand cycles of repeated loading. Since concrete pavements are usually un-reinforced, concrete is expected to endure flexural tension stress in such structures. Consequently, understanding the fatigue behaviour in tension is also needed. Serious fatigue problems are also encountered in shell panel/plate structures.

Much attention has been paid by researchers in recent years to fatigue problems. There are many reasons behind this increasing interest. New types of materials such as fiber reinforced concrete and high-strength concrete have been used in civil engineering structures, but little is known of their long-term performance. Some structures such as marine structures are usually subjected to wind and wave repeated loading. There is increasing recognition that the effects of cyclic loading on the behaviour of the materials may be significant under service loading, even if the repeated loading does not cause a fatigue failure.

A number of researches have been performed in the past to evaluate the fracture or the fatigue performances of plain concrete (see Refs. [3,4]). Fiber reinforced concretes are structural materials developed through extensive research and development during the last two decades. The toughness and strength improvements in paste and mortar reinforced by carbon fiber 6–10 mm in length were researched by Banthia and Sheng [5,6]. In Banthia's study, the test results shown that cement-based matrices reinforced at 1%, 2%, 3% by volume of carbon fiber, an increase in fiber content led not only to an increase in load carrying capacity but also led to toughness. Barzin and Li [7] have studied the tensile and flexural properties of cementations composites

* Tel.: +86-10-67395515; fax: +86-10-67391980.
E-mail address: dengzc@bjpu.edu.cn (Z. Deng).

0958-9465/$ - see front matter © 2004 Elsevier Ltd. All rights reserved.
doi:10.1016/j.cemconcomp.2004.03.002

reinforced with carbon fiber, and the lower efficiency observed in the tests may be attributed to the carbon fibers with short length (length = 1 mm). This paper reports on a study, which is part of an investigation into the fatigue reliability of concrete reinforced with longer length (length = 25 mm) carbon fibers. The supplier recommends the addition of only a small quantity, 0.1–0.3% by volume. There is a need to know whether there are other changes in the fracture properties of concretes reinforced with carbon fibers with such small volume fraction. In particular, it is important to know whether there is any change in the fatigue life of the material and fracture mode. There is also paucity of information regarding the flexural fatigue behaviours and endurance limit of concretes reinforced with carbon fibers.

Carbon fiber reinforced concrete is now being used in civil engineering projects, such as projects pavements, bridge decks, and so on. Carbon fiber reinforced concretes are reliable structural materials with superior performance characteristics compared to conventional concrete. The addition of carbon fiber in concrete has been found to improve several of its properties, primarily cracking resistance, ductility and fatigue life.

However, fracture and fatigue behaviour of carbon fiber reinforced concrete has not been paid much attention by researchers and users. The primary purposes of this study were

1. To determine the fracture mechanics properties of carbon fiber reinforced concrete.
2. To understand the influence of preliminary cyclic loading on the fracture behaviour of carbon reinforced concrete.
3. To evaluate the fatigue performance and fatigue damage accumulation of carbon fiber reinforced concrete with cracks.

2. Materials and specimens

2.1. Materials, and mix proportions [8]

Portland cement was used for all mixes. The fine aggregate used was natural sand with maximum particle size of 3.5 mm; the coarse aggregate used was natural stone, having a maximum particle size of 20.5 mm.

The carbon fiber was monofilament, with an elastic modulus of 230 GPa, and a tensile strength of 3.45 GPa. The fiber length was 25 ± 2 mm, and the fiber volume fraction was varied from 0.1% to 0.3%.

The water-to-cementitious solids ratio used for all mixes was 0.34. All mixes contained 410 kg/m^3 of cement, 1246 kg/m^3 of coarse aggregate, 593 kg/m^3 of sand, 13 kg/m^3 of silica fume and 0.94 kg/m^3 of superplasticizer.

2.2. Mixing, casting and curing

The flexibility of the mixing chamber allows the breakup of the fiber and contributes to the mixing action, while a vigorous shearing action distributed the fibers homogeneously.

In the mixing procedure, fiber and the fine and coarse aggregate were first mixed together with 2/3 of the required water and mixing was continued for 3 min. Next the cement and silica fume were added followed by the reminding 1/3 of the water with the super-plasticizer mixed in. Thereafter, the mixing was continued for a further 3 min. After casting and finishing the surface, the specimens were covered with a plastic sheet and cured for 24 h at room temperature. They were then removed from the mould and placed in water maintained at 23 °C until the beginning of the tests. Because of the large number of specimens and time needed for fatigue testing, all of the specimens were water cured for at least 90 days, and when the specimens were moved out of water the surface was coated with paraffin wax to minimize the effects of age and moisture loss on the test results. A water-cooled diamond blade circular saw was used to cut a 30-mm notch (width about 4-mm) at mid-span of the specimens for the three point bending tests.

2.3. Specimens

The following specimens were cast from each mix: six cubes $150 \times 150 \times 150$ mm for compressive strength, six beams $150 \times 150 \times 450$ mm with notch for static fracture testing, and six beams $150 \times 150 \times 450$ mm with notch for each stress ratio of the preliminary cyclic loading tests or the flexure fatigue tests.

The shape and size of the beam specimens is shown in Fig. 1. A total of 186 beams, as shown in Table 1, were used in the testing programme.

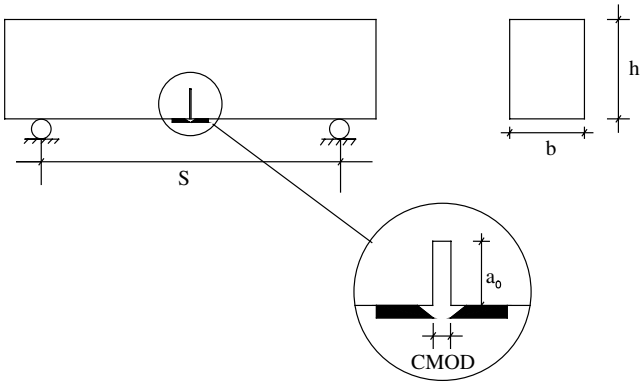

Fig. 1. Geometry of beam in flexure test.

Table 1
Test specimens

Specimen designation	Fiber percent by volume	Number of specimens			
		Cubes	Beams		
			Static fracture	Preliminary cyclic	Fatigue
C	0	6	6	36	18
CF1	0.1	6	6	18	18
CF2	0.2	6	6	18	18
CF3	0.3	6	6	18	18

3. Experimental programme

The experimental programme was designed to evaluate the fracture parameters and to study the flexure fatigue behaviour of carbon fiber reinforced concrete.

3.1. Slump and compressive strength

The freshly mixed concrete was tested for slump (ASTM C143). Cube specimens were tested for compressive strength at 28 days, six specimens for each mix, according to ASTM C39.

3.2. Static fracture parameters testing method

The three point bending beams with a central notch were used for determining the static fracture parameters. All of the fracture and flexural fatigue tests were carried out in an Instron 8502 universal testing machine with a closed-loop control system.

The deflection of the loading point at the middle was measured using two standard dynamic Instron extensometers type 2620, with 12.5 mm gauge length, fitted on each side of the specimen on a special measuring device. This special device, as shown in Fig. 2, is the so called Japan Yoke deflection measuring method, and the deflection data was used as the feedback signal to control the loading process. The loading process was controlled by a constant deflection rate of 0.010 mm/min. The crack mouth opening displacement was measured using a displacement sensor, LVDT, as shown in Fig. 2.

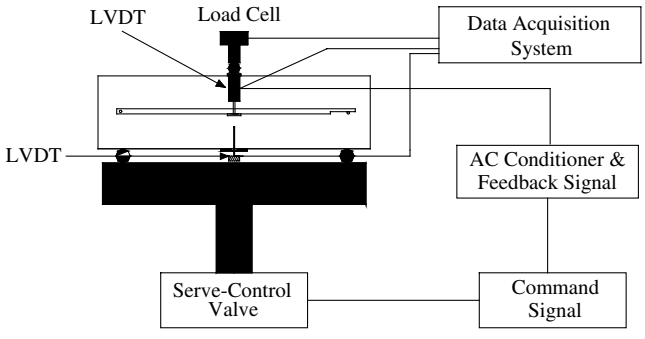

Fig. 2. Schematics of flexural test setup.

Before measuring the complete load–deflection curves for the test specimens, loading/unloading tests were performed in order to obtain the initial (C_i) and unloading compliance (C_u) value. The applied load was manually reduced when the load just passes the maximum load and was approximately 95% of the peak load. When the applied load was reduced to zero, reloading was applied. Each loading and unloading cycle was finished in about 2 min.

The stress strength factor is determined based on an effective crack approach using principles of linear elastic fracture mechanics. The loading/unloading curves were used to calculate the unloading compliance C_u of the specimen at various CMOD levels. The critical effective crack length was obtained by matching the unloading compliance with the initial compliance through solving the following nonlinear equation. The analysis of this test results is based on the earlier work of Shah [4]

$$E = 6S(a_0 + \Delta a)V_1(\alpha)/[C_u h^2 b] \quad [\mathrm{N\,m^{-2}}] \tag{1}$$

in which C_u is the unloading compliance obtained from load–CMOD curve; also

$$V_1(\alpha) = 0.76 - 2.28\alpha + 3.87\alpha^2 - 2.04\alpha^3 + \frac{0.66}{(1-\alpha)^2} \tag{2}$$

$$\alpha = \frac{a_0 + \Delta a}{h} \tag{3}$$

where S, h and b represent the span, depth and specimen thickness, respectively. a_0 and Δa are the initial notch length and incremental crack growth. E represents the effective Young's modulus obtained from the initial compliance of the specimen. By measuring the peak load F_{max} and $a = a_0 + \Delta a$ at successive intervals of crack growth, the stress intensity factor at the tip of the critical effective crack can be obtained by

$$K_{Ic}^{e} = 3F_{max}\frac{S\sqrt{\pi a}F(\alpha)}{2h^2 b} \tag{4}$$

in which

$$F(\alpha) = \frac{1.99 - \alpha(1-\alpha)(2.15 - 3.93\alpha + 2.7\alpha^2)}{\sqrt{\pi}(1+2\alpha)(1-\alpha)^{3/2}} \tag{5}$$

The critical crack tip opening displacement $CTOD_c$ is determined using equation

$$\mathrm{CTOD_c} = \frac{6F_{\max}SaV_1(\alpha)}{Eh^2b}[(1-\beta)^2 + (1.081 - 1.149\alpha)(\beta-\beta^2)]^{1/2} \quad [\mathrm{m}] \tag{6}$$

where $\alpha = a/h$, $\beta = a_0/h$.

In the present study, toughness is quantified by the fracture energy denoted as G_F, which is the energy required to create one unit area of crack surface. G_F was calculated by RILEM proposal [9]. W_0 the total energy supplied to break the specimen completely is measured using the load–deflection curves of the fracture test. The G_F is calculated using

$$G_F = (W_0 + mg\delta_0)/A \tag{7}$$

where $mg\delta_0$ is the energy produced by the specimen weight (m is the specimen mass, g is the gravitation acceleration, and δ_0 is the maximum deflection of beam at peak load), and A is the crack path area.

3.3. Pre-loading testing method

According to Ref. [10], the influence of preliminary cyclic loading on fracture mechanics parameters and deformation behaviour mainly depend upon the stress level and the first several counts of cyclic loading, and the influence significantly decreases with cyclic counts, so the number of preliminary cyclic loading was set at 20 in this present study. The specimens were firstly subjected to the required cyclic loading before the final fracture test. A varying maximum load level, given by

$$s = \frac{F_{\max}^{\text{fatigue}}}{F_{\max}^{\text{static}}} \tag{8}$$

was used in the preliminary cyclic loading and fatigue test programme.

For the preliminary cyclic loadings, the stress ratios s were 0.6, 0.65, 0.7, 0.8 and 0.9 for plain concrete, and 0.7, 0.8 and 0.9 for fiber reinforced concrete. The preloading tests were all controlled by a constant load rate of 10 N/s using a sinusoidal wave form with a frequency of 2 Hz. After finishing the preliminary cyclic loading test, the same specimens were used again to do the quatic-static fracture test. Thus, by measuring loading/unloading compliance and the complete load–deflection curves, the critical effective crack length and the subsequent fracture toughness and fracture energy can be determined. The comparison of its behaviour with that of the reference specimens allows us to obtain the loading history influence.

3.4. Fatigue fracture testing method

The fatigue fracture tests were carried out in load control using a sinusoidal wave form with a frequency of 2 Hz. A constant load ratio R between minimum and maximum load levels

$$R = \frac{F_{\min}}{F_{\max}} = 0.1 \tag{9}$$

and a varying maximum load level s were used in the present test programme.

The following stress ratios s were selected: 0.65, 0.70, 0.8, and 0.9 for plain concrete and 0.7, 0.8 and 0.9 for composite with carbon fibers. A program was written specifically for the purpose of this investigation. The input data for the program include the maximum number of cycles, maximum load amplitude, number of load cycles per second, and number of data points per load cycle. In addition to actively controlling the test until failure, the program was used to calculate the energy dissipated during each load cycle. This energy was evaluated numerically as the area under the load–deflection curves. The program automatically sums the energy absorbed during all cycles until failure. Each loading/unloading cyclic curve was used to calculate the unloading compliance C_u of the specimen at various CMOD levels and to determine the critical effective crack length at each cycle.

4. Results and discussions

4.1. Static fracture test

The carbon fibers used in this programme performed very well. The mixing action spread the fibers uniformly throughout the concrete. The concrete seemed to be easy to work with. Even though there was an apparent reduction in slump, the concrete was much more workable than a plain mix of corresponding slump with super-plasticizer. It can be seen, from Table 2, that the carbon fiber has no effect on the compressive strength of concrete.

Average static fracture parameters are summarized in Table 3. In addition to the maximum load, the CMOD and deflection at peak load, the loading/unloading compliance of the specimen, the critical effective crack

Table 2
Slump and compressive strength

Specimen designation	Slump (mm)	Compressive strength (MPa)
C	128	31.9 (10.3)
CF1	74	27.3 (9.5)
CF2	65	28.1 (13.2)
CF3	21	29.5 (9.8)

Note: Values in parentheses represent coefficient of variation (100%), in lower tables are the same mean.

Table 3
Static fracture parameter

Specimen designation	F_{max} (kN)	CMOD at peak load (mm)	Deflection at peak load (mm)	$C_i \times 10^{-6}$ (mm/N)	$C_u \times 10^{-6}$ (mm/N)	a/h	$K^e_{Ic,s}$ (MPa $\sqrt{m}$)	$G_{F,s}$ (N/m)	$CTOD_{c,s}$ (mm)
C	2.76 (8.9)	0.201 (53.7)	0.0253 (55.7)	6.05 (9.9)	10.10 (5.6)	0.34 (6.5)	0.743 (14.3)	141.4 (19.0)	0.034 (35.3)
CF1	3.58 (5.3)	0.22 (21.8)	0.0310 (36.8)	7.28 (5.0)	16.90 (3.6)	0.46 (7.0)	1.35 (14.9)	296.2 (12.7)	0.069 (14.5)
CF2	4.01 (4.3)	0.238 (26.1)	0.0341 (35.5)	6.98 (4.9)	17.70 (1.9)	0.51 (4.7)	1.74 (18.0)	331.1 (12.4)	0.100 (41.0)
CF3	4.45 (4.6)	0.245 (24.5)	0.0386 (27.2)	6.74 (4.6)	18.69 (2.0)	0.55 (4.9)	2.27 (18.8)	364.7 (9.9)	0.144 (41.7)

length a, fracture energy $G_{F,s}$ and critical stress intensity factor $K^e_{Ic,s}$ and critical crack tip opening displacement $CTOD_{c,s}$ for all specimens are also reported. In all tables and equations the below-script 's' denote the static fracture parameters. The results of the critical effective crack length, as shown in Table 3, indicate that fracture mechanisms of composites with fiber is similar to plain concrete, and that the critical effective crack growth length of fiber reinforced concrete is significantly larger than in plain concrete, e.g. the critical effective crack length of the specimen CF2 with 0.2% carbon fibers is 1.5 times larger than that of plain concrete. The higher the fiber content, the larger is the critical effective crack length. Carbon fibers were shown to stabilize the cracks and increase the critical effective crack length, and provide a significant bridging force to delay the crack rapidly opening. The fiber reinforced concrete shows a significantly larger fracture process zone than that of plain concrete.

Note that, as shown in Table 3, the test results of static fracture parameters $K^e_{Ic,s}$, $G_{F,s}$ and $CTOD_{c,s}$ are increased by the addition of fibers and are significantly increased with fiber volume fraction, e.g., for the composite with 0.3% carbon fiber the critical stress intensity factor $K^e_{Ic,s}$ and fracture energy $G_{F,s}$ are 3.0 and 2.6 times larger than that of plain concrete respectively. Composites exhibit a ductile behaviour since the fiber pullout generates a significant closing force in the crack surface. Fiber debonding and pullout seem to be significant since the long length of fiber can provide significant bridge length across the crack faces. The higher efficiency observed in the present study, may be attributed to the length of fibers being longer than the average aggregate size.

In Banthia's study, peak load and effective fracture toughness of mortar reinforced with 3% carbon fibers 6 mm in length were about 2 and 10 times higher than cement mortar, respectively. Those values in present tests were 1.6 and 3 times higher than the plain concrete. The lower efficiency observed in the present study may be due to concrete with lower fiber volume fraction than in Banthia's study [5].

4.2. Preliminary cyclic loading tests

The influence of preliminary cyclic loading on the fracture parameters and deformation behaviour of plain concrete and carbon fiber reinforced concretes are summarized in Tables 4 and 5 whereas the a the critical

Table 4
Influence of preliminary cyclic loading on the fracture behaviour for plain concrete

Stress level	F_{max} (kN)	CMOD at peak load (mm)	Deflection at peak load (mm)	$C_i \times 10^{-6}$ (mm/N)	$C_u \times 10^{-6}$ (mm/N)	a/h	K^e_{Ic} (MPa $\sqrt{m}$)	G_F (N/m)	$CTOD_c$ (mm)
0.60	2.762 (11.8)	0.201 (58.7)	0.0253 (55.7)	6.05 (6.0)	10.1 (2.7)	0.335 (7.1)	0.743 (11.3)	142.1 (19.0)	0.036 (47.2)
0.65	2.66 (10.7)	0.188 (50.5)	0.0241 (48.5)	6.18 (4.1)	10.2 (3.0)	0.337 (8.6)	0.717 (15.6)	138.8 (21.3)	0.035 (35.4)
0.70	2.54 (12.1)	0.162 (38.6)	0.0226 (58.4)	6.23 (8.3)	10.6 (3.9)	0.350 (10.1)	0.691 (11.8)	132.5 (13.7)	0.0312 (44.9)
0.80	2.46 (10.9)	0.150 (48.7)	0.0210 (44.8)	6.81 (8.8)	9.9 (3.6)	0.327 (13.0)	0.665 (7.7)	127.7 (16.8)	0.0314 (49.0)
0.90	2.298 (6.6)	0.132 (51.2)	0.2030 (30.7)	6.44 (6.9)	10.4 (2.3)	0.343 (5.9)	0.621 (17.02)	122.0 (26.1)	0.0284 (52.5)

Table 5
Influence of preliminary cyclic loading on the fracture behaviour for fiber reinforced concrete

Specimen designation	Stress level	F_{max} (kN)	CMOD at peak load (mm)	Deflection at peak load (mm)	$C_i \times 10^{-6}$ (mm/N)	$C_u \times 10^{-6}$ (mm/N)	a/h	K_{Ic}^e (MPa $\sqrt{m}$)	G_F (N/m)	$CTOD_c$ (mm)
CF1	0.7	3.30	0.201	0.02910	7.94	16.7	0.459	1.252	291.07	0.064
		(19.7)	(52.2)	(42.6)	(3.0)	(6.7)	(3.4)	(9.1)	(12.5)	(57.8)
	0.8	3.12	0.197	0.0284	8.01	16.5	0.453	1.162	287.27	0.058
		(14.6)	(23.3)	(45.8)	(7.0)	(4.6)	(4.6)	(7.8)	(20.6)	(53.4)
	0.9	2.94	0.144	0.0269	8.08	17.0	0.467	1.140	278.93	0.060
		(13.6)	(37.3)	(34.2)	(7.6)	(5.4)	(6.9)	(8.3)	(15.8)	(31.7)
CF2	0.7	3.92	0.220	0.0331	6.81	16.9	0.4988	1.700	323.05	0.091
		(13.0)	(41.0)	(32.0)	(6.4)	(3.3)	(5.4)	(8.3)	(12.2)	(44.4)
	0.8	3.77	0.201	0.0319	6.90	17.4	0.4990	1.641	310.2	0.0894
		(13.2)	(36.6)	(37.6)	(7.4)	(3.6)	(12.2)	(6.3)	(17.7)	(37.2)
	0.9	3.63	0.188	0.0286	6. 89	17.9	0.4997	1.578	296.0	0.0899
		(16.1)	(25.1)	(34.3)	(3.6)	(4.7)	(5.8)	(8.6)	(12.7)	(45.7)
CF3	0.7	4.36	0.215	0.0374	6.81	18.45	0.5601	2.230	357.0	0.137
		(13.6)	(16.8)	(29.4)	(5.2)	(5.7)	(4.5)	(9.6)	(13.5)	(37.8)
	0.8	4.24	0.179	0.0354	7.21	17.98	0.5599	2.166	346.5	0.139
		(11.4)	(43.9)	(29.7)	(3.8)	(2.9)	(11.2)	(9.1)	(16.2)	(16.8)
	0.9	4.10	0.156	0.0310	7.15	18.46	0.5612	2.091	331.5	0.1297
		(14.9)	(24.3)	(52.3)	(4.8)	(1.4)	(6.1)	(15.1)	(8.9)	(32.4)

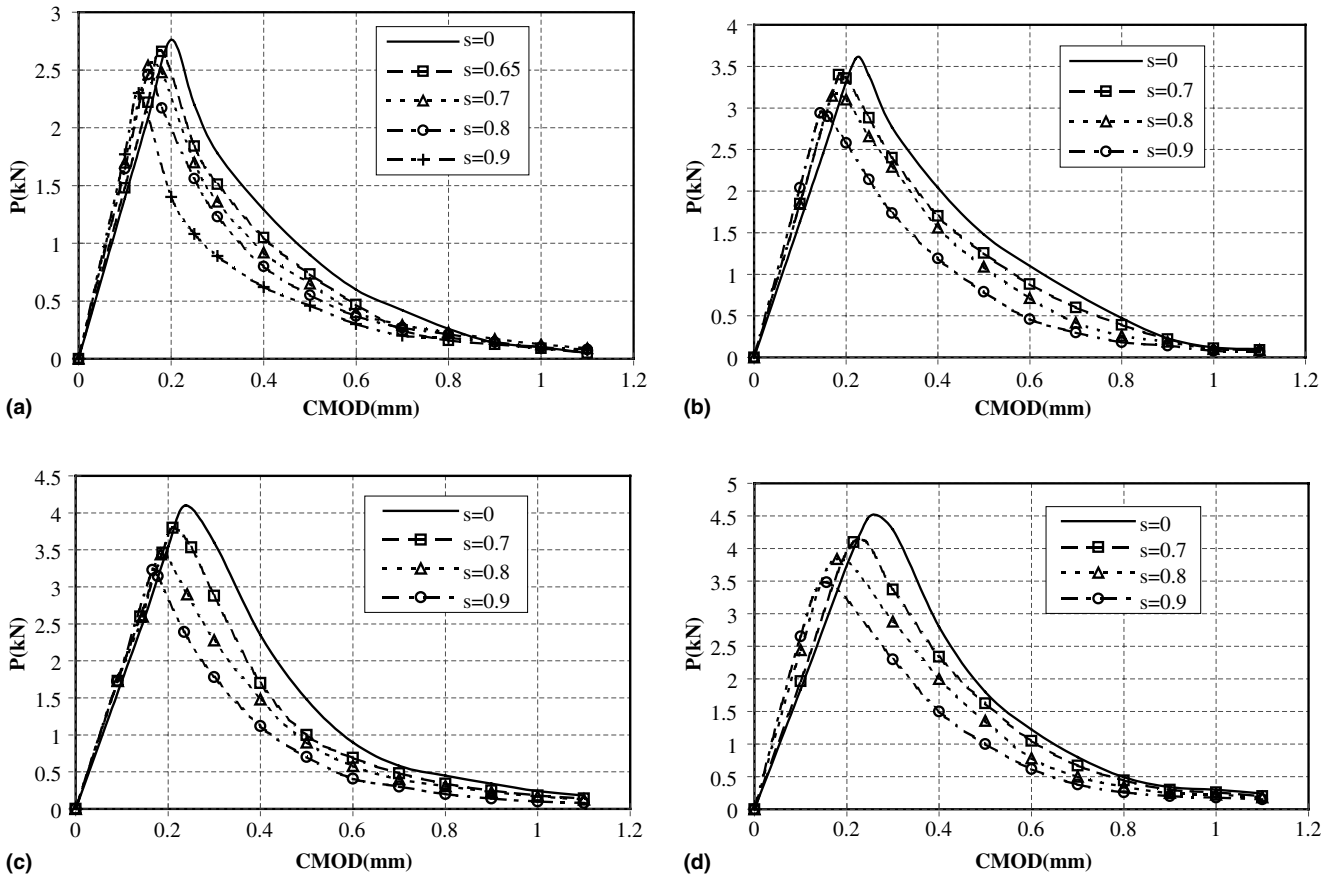

Fig. 3. Load–crack tip opening deformation curves after 20 cycles of pre-loading for concrete with and without fibers. (a) Plain concrete; (b) CF1; (c) CF2; (d) CF3.

effective crack length ($a = a_0 + \Delta a$ at successive intervals of crack growth). The load–COMD curves after 20 cycles of pre-loading for different stress ratios are plotted in Fig. 3(a)–(d). In Tables 4 and 5, K_{Ic}^e and G_F are the

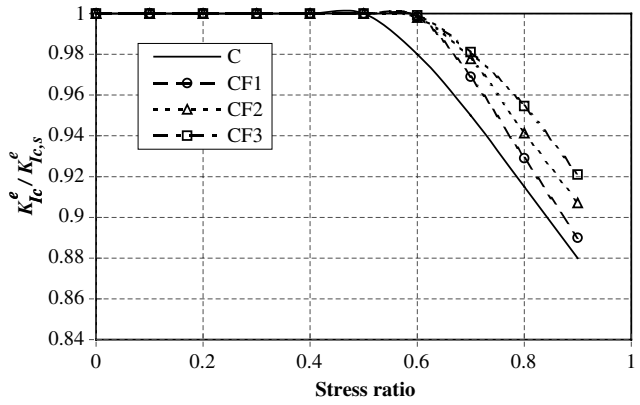

Fig. 4. Variation of K_{Ic}^{e} in the terms of the pre-loading level after 20 cycles.

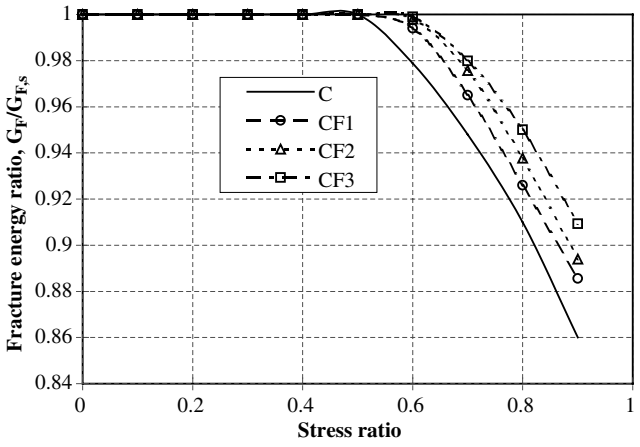

Fig. 5. Variation of G_F in the terms of the pre-loading level after 20 cycles.

subsequent fracture toughness and fracture energy when specimens were subjected to pre-loading (Figs. 4 and 5). The following conclusions can be drawn from test results:

1. After the preliminary cyclic loading, the stiffness of the test specimens increase, which is reflected by an increase of slope of the curves $F = f(\mathrm{CMOD})$. Such a phenomenon indicates that there is an increase of the elastic E, and the material become more brittle. It can be seen that due to the preliminary cyclic loading test, the crack opening displacement and deflection at the peak load are lower than the static fracture test results, and the higher the pre-loading stress levels, the lower the crack opening displacement and deflection at the peak load. This may be due to the irreversible deformation in the preliminary cyclic loading process which increases with the pre-loading stress ratios.
2. For plain concrete, if the stress ratio is not larger than 0.65, the F_{max} is not influenced by the pre-loading history. However, if the stress ratios were larger than 0.65, the F_{max} reduced, and decreased with the increasing stress levels, especially, when the stress ratio is 0.9, the F_{max} decreased noticeably compared with the quasi-static results. For fiber reinforced concrete, this influence threshold value increase up to 0.7, and, the higher the stress ratios of preliminary cyclic test, the lower the subsequent peak load.
3. The fracture parameters were noticeably reduced if the pre-loading strength is higher than a certain threshold for both plain concrete and fiber reinforced concrete. When the stress ratio is larger than 0.65 and 0.7, the fracture energy and critical stress strength factor of plain concrete and carbon fiber reinforced concrete are lower than that of the static test results respectively. For a given fiber volume fraction, the higher the stress ratio of pre-loading test, the lower will be the subsequent fracture parameters. For a given stress ratio, the higher the fiber volume, the smaller the reduction of fracture energy. Concrete reinforced with higher fiber volume, the damage accumulation rate of pre-loading cycle is slower than that of specimens with lower fiber content, i.e., specimens with higher fibers content can delay the fracture damage process. The influence of pre-loading history on the fracture energy is significantly greater than in the case of fracture toughness.
4. The critical effective crack length is not influenced by the pre-loading cycle, i.e., the critical effective crack propagation length is mainly the same as in the static test results.

4.3. Fatigue fracture testing results

4.3.1. Fatigue life

Table 6 summarizes the numbers of cycles to failure for all cyclically tested specimens. These data are also plotted in Fig. 6(a)–(c) for plain and carbon fiber reinforced concrete beams, respectively, which show the number of cycles to failure as functions of fiber content for the given stress levels. From the test results, one can see that carbon fiber has a clearly beneficial effect on the fatigue life of concrete, and this increases with the value of addition fiber fraction, e.g., specimen CF3 is 1.3 times larger than that of CF1 when the stress ratio is 0.9. The higher the fiber content, the larger will be the counts of cycles to failure.

4.3.2. Energy consumed during fatigue test

The area of curve under the load–deflection response is a measure of the total energy consumed/absorbed during fatigue/fracture testing. During the cycle process, the energy dissipated during each loading cycle was computed and saved. Table 7 summarizes the total

Table 6
Number of cycles to failure N_f

Stress ratio	Specimen no.	Test specimens			
		C	CF1	CF2	CF3
0.70	1	49	108	121	169
	2	78	141	164	201
	3	94	128	121	184
	4	58	120	125	202
	5	92	111	110	165
	6	87	124	142	207
	Mean	76.3	122	130.5	188
	COV	24.6	9.9	14.9	9.6
0.8	1	36	97	104	129
	2	59	103	118	105
	3	65	99	124	121
	4	38	108	99	129
	5	42	84	121	113
	6	63	75	108	121
	Mean	51	94.3	112.3	119.7
	COV	26.2	13.2	9.0	7.8
0.9	1	19	69	59	102
	2	21	57	72	69
	3	30	64	61	86
	4	31	86	56	93
	5	35	61	58	81
	6	43	49	63	77
	Mean	30	64	61.5	84.7
	COV	29.8	20.0	9.2	14.0

energy dissipated by each beam by the time fracture failure occurred, i.e., the beam's total energy dissipation capacity. The relation between total energy dissipated and the fiber content are shown in Fig. 7(a)–(c). The value of total energy absorption is dependent on the fatigue life, and the larger the fatigue life, the higher energy will be consumed by the specimen. The energy consumed for a composite with fibers is dramatically larger than for the control concrete, and the higher the fiber volume fraction, the larger will be the total energy dissipated. The total energy consumed by the composite with 0.3% fibers was 13.7 times larger than for the control concrete, when the stress level was 0.9. Such a clearly beneficial behaviour may be attributed to the carbon fiber with longer length when compared to the test results of Barzin and Li [7].

The energy absorption capacity almost noticeably decreased with increasing stress level, i.e., the lower the stress level, the larger will be the total energy dissipated. At higher stress levels, the first few cycles of fatigue life initiate the mortar cracking, and the stress intensity at the crack tip is normally enough to overcome the resistance of fibers, if they are present. At lower stress levels, the fracture damage process starts debonding cracks and mortar crack initiation occurs. If the fiber's resistance force exceeds the stress intensity the crack would be stopped, and more load cycles are needed to let the crack run across fibers. Thus, at lower stress

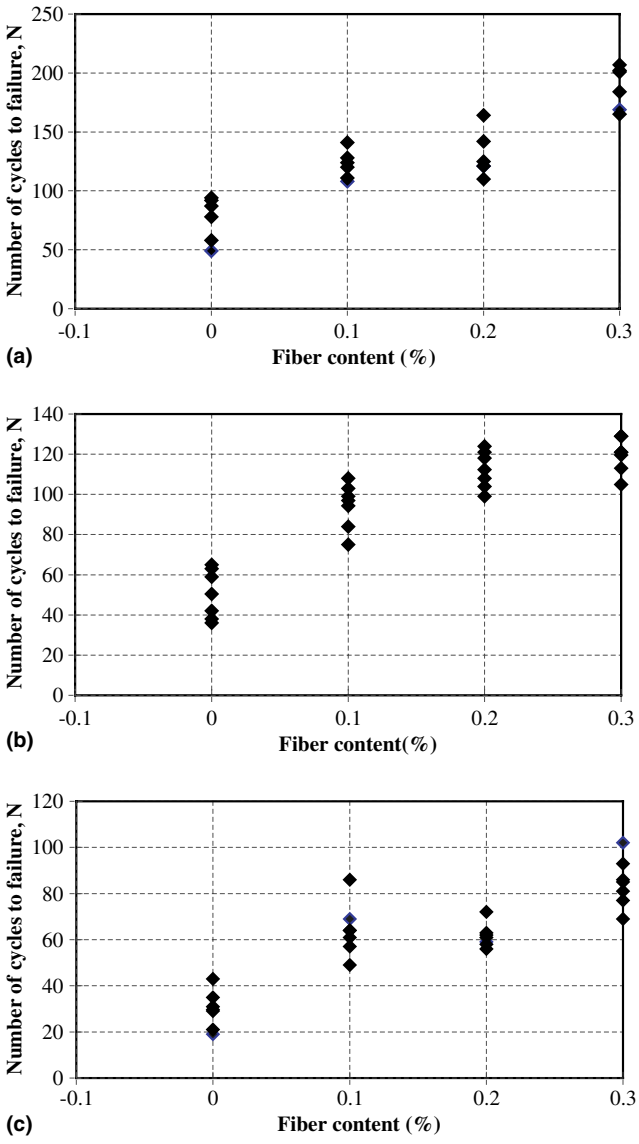

Fig. 6. Number of cycles to failure as a function of carbon fiber content. Stress ratio is (a) 0.7; (b) 0.8; (c) 0.9.

levels, in addition to the bond cracking, there is more efficient resistance provided by the fibers and as a result the amount of dissipated energy increases.

4.3.3. Damage accumulation

The histograms of energy dissipation, normalized with regard to total energy absorption capacity, are defined as fatigue damage index D, i.e.,

$$D = \frac{E}{E_{\text{tot}}} \tag{10}$$

The damage index is shown as a function of cycle ratio N/N_f, where N_f is the number of cycle to failure and N is the number of cycles actually applied, both for the stress level s indicated in Fig. 8(a)–(d) respectively. Also shown in each graph for comparison is a straight line, corre-

Table 7
Total dissipated energy E_{tot} (N m)

Stress levels	Specimen no.	Test specimens			
		C	CF1	CF2	CF3
0.70	1	1.40	10.92	10.60	12.60
	2	1.34	10.7	11.0	15.1
	3	1.10	11.3	10.9	15.4
	4	1.56	9.7	13.1	13.8
	5	1.78	12.1	11.4	15.1
	6	1.57	10.2	12.5	14.2
	Mean	1.46	9.4	11.6	14.37
	COV	16.0	7.8	8.6	7.4
0.8	1	1.1	8.7	7.1	11.6
	2	1.4	9.4	8.7	10.5
	3	1.8	8.1	9.2	11.9
	4	0.9	7.8	10.2	13.2
	5	1.2	8.1	12.1	11.0
	6	1.08	7.4	9.7	13.8
	Mean	1.25	8.25	9.5	12.0
	COV	25.4	8.6	17.5	10.6
0.9	1	0.47	7.1	7.8	9.8
	2	1.1	7.3	7.9	10.1
	3	0.75	6.9	8.1	9.4
	4	0.71	7.0	7.4	11.0
	5	0.69	8.4	8.2	9.7
	6	0.77	5.8	9.1	9.4
	Mean	0.75	7.08	8.08	9.9
	COV	27.2	11.8	7.01	6.1

sponding to Miner's rule of linear damage accumulation [11]. Each curve represents the average of six individual beams tested for each case. Because of the small number of samples per data point, the following conclusions should be considered with caution.

1. Miner's rule, which presumes a linear accumulation of damage, is not generally applicable for plain and fiber reinforced concrete beams with a central notch. All results exhibit a more or less pronounced nonlinear evolution of damage. The degree of nonlinearity increases almost consistently with stress ratio. During the stable crack opening process, the damage accumulation increases almost proportionally with the number of cycles actually applied. However, the damage accumulation accelerates as the beams approaches failure. The damage accumulated curves for plain and fiber reinforced concrete beams deviate markedly from linearity, for stress levels in excess of 0.7 and 0.8, respectively.
2. For a given stress ratio, the higher the fiber content, the lower will be the rate of damage accumulation. With larger fiber content more fibers available to bridge the crack and provide added ductility and energy absorption capacity. Carbon fiber can transfer more loads, thereby delaying the process of debonding and pullout and improving the composite behaviour under cyclic loading.

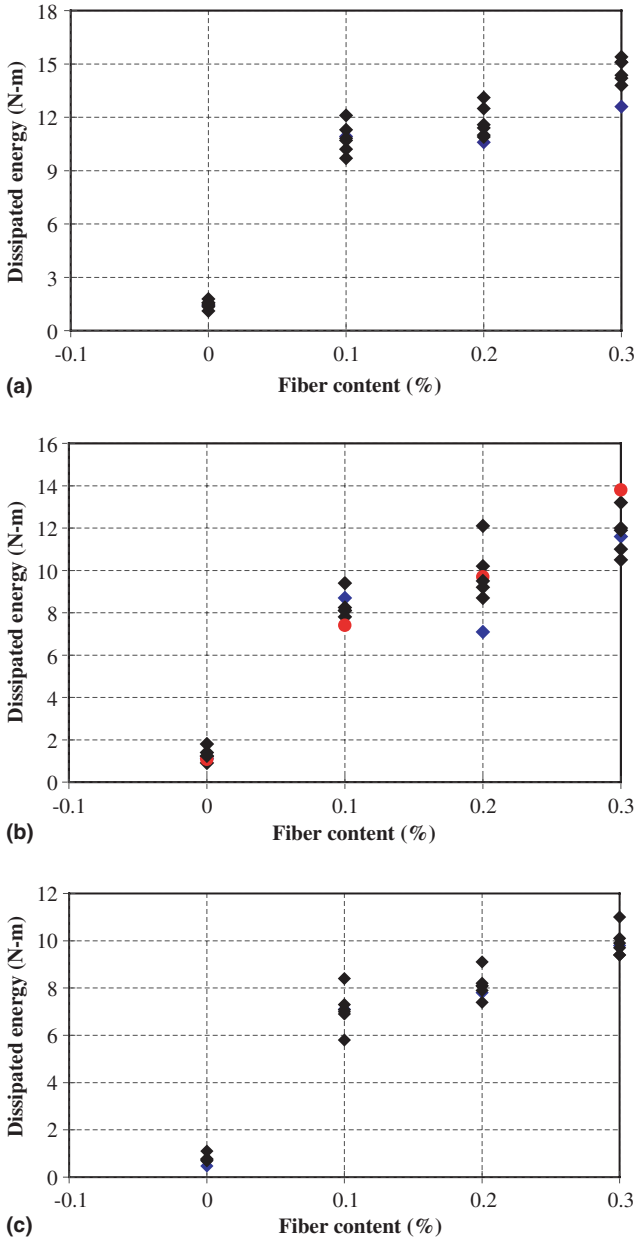

Fig. 7. Dissipated energy as a function of carbon fiber content. Stress ratio is (a) 0.7; (b) 0.8; (c) 0.9.

5. Conclusions

1. The fracture parameters K_{Ic}^{e} and $CTOD_c$ will be noticeably reduced if the preliminary cyclic loading capacity is greater than a certain threshold, and the threshold for carbon fiber reinforced concrete is about 70% of static fracture strength.
2. The flexural fatigue life of carbon fiber reinforced concrete beam with a central notch is much larger than that of the matrix, i.e., fatigue life of carbon fiber reinforced concrete with maximum volume fraction of 0.3% is about 2.8 times higher than that of plain concrete when the fatigue stress level is 0.9.

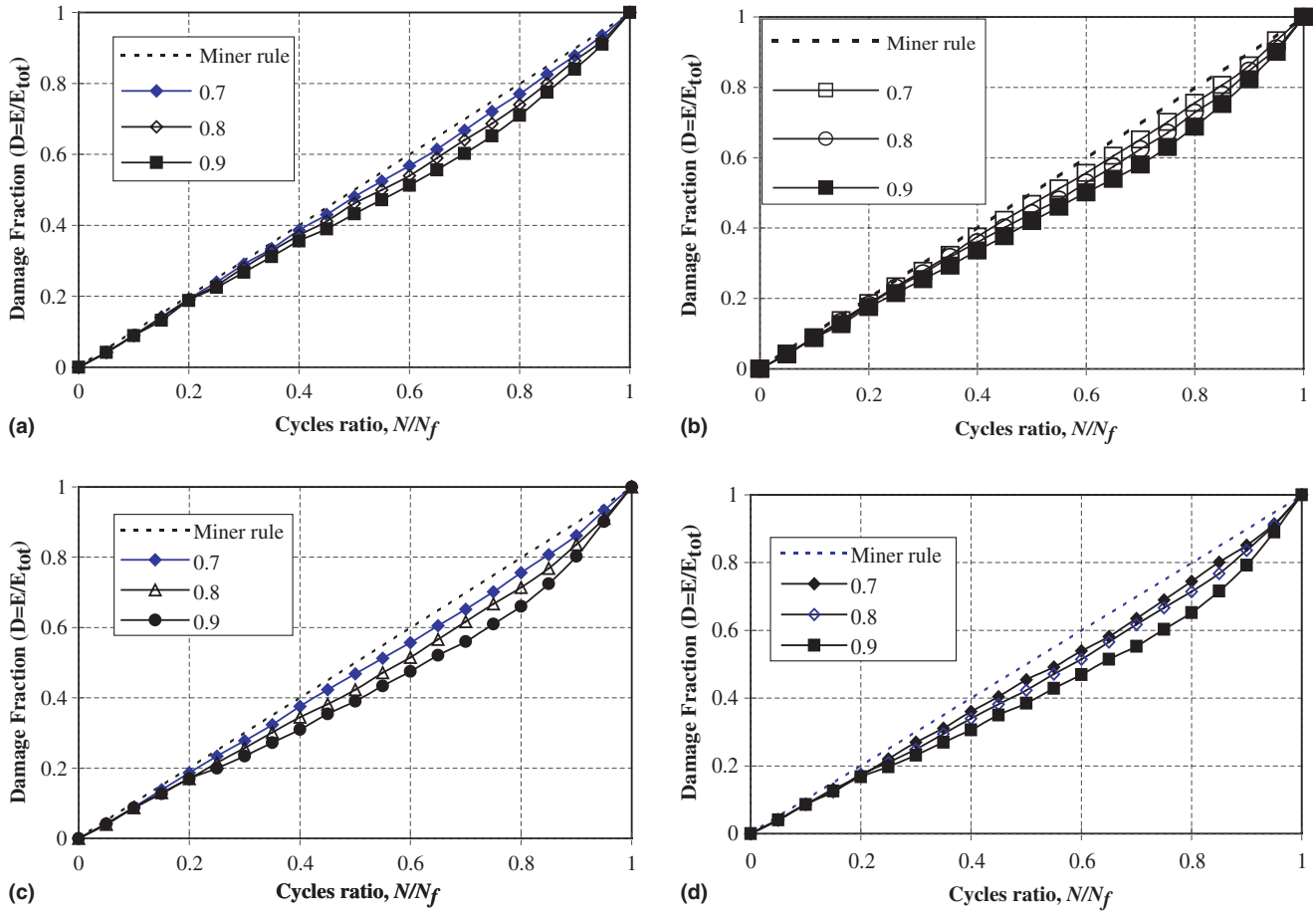

Fig. 8. Dissipated energy as a function of carbon fiber content. (a) Plain concrete; (b) CF1; (c) CF2; (d) CF3.

3. The critical effective crack length is independent of the fatigue life for both plain and fiber reinforced concrete.
4. The total energy dissipated values for carbon fiber reinforced concrete specimens are 9.6–13.7 times larger than that of plain concrete during the flexure fatigue/fracture tests.
5. The histograms of energy dissipation, normalized with regard to total energy absorption capacity, can be used as a fatigue damage index. The damage accumulated curves in flexure for plain and fiber reinforced concretes deviate markedly from linearity for stress levels in excess of 0.7 and 0.8, respectively.

Acknowledgements

This work was supported by a grant from the Natural Science Foundation of China, grant no. 50378006.

References

[1] Rescher OJ. Importance of cracking in concrete dam. Eng Mech 1990;35(1):23–9.
[2] Pons G, Ramoda SA, Maso JC. Influence of the loading history on fracture mechanics parameters of micro-concrete: effects of low-frequency cyclic loading. ACI Mater J 1988;(5): 341–6.
[3] Swamy RN. Fracture mechanics applied to concrete. In: Lydon FD, editor. Development in concrete technology-1. Applied Science Publishers Ltd; 1979. p. 221–81.
[4] Shah SP. Determination of fracture parameters of plain concrete using three-point bend tests. Mater Struct 1990;23:457–60.
[5] Banthia N, Sheng J. Fracture toughness of micro-fiber reinforced cement composites. Cem Concr Compos 1996;18:251–69.
[6] Banthia N, Moncef A, Sheng J. Uni-axial tensile response of cement composites reinforced with high-volume fraction of carbon, steel, and polypropylene micro-fibers thin reinforce concrete products and system, SP-146. In: Balaguru, editor. American Concrete Institute; 1994. p. 43–68.
[7] Barzin M, Cheng YL. Mechanical properties of hybrid cement based composites. ACI Mater J 1996;93(3):284–92.
[8] Deng Z. The fatigue behavior of carbon fiber reinforced concrete. PD, Zhejiang University, 2000.
[9] RILEM Committee 50-FMC. Determination of the fracture energy of mortar and concrete by means of three-points bend test no notched beams. Mater Struct Res Testing (RILEM, Paris) 1985;18(106):285–90.
[10] Lin G, Zhou HT, Huang CK. Experimental study of effect of cyclic loading history on the fracture properties of concrete. J Hydraulic Eng 1994;(5):25–9 [in Chinese].
[11] Noquchi. Miner's rule for fatigue life of short carbon fiber reinforced poly-ether-ether-ketone. J Soc Mater Sci Japan 1994; 43(489):672–8.